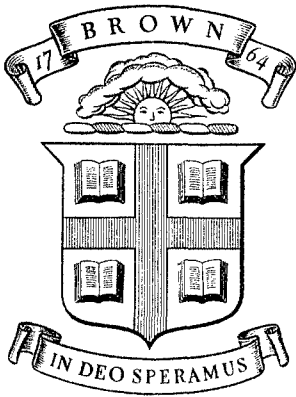


BU  
ARPA-E-53



Division of Engineering  
BROWN UNIVERSITY  
PROVIDENCE, R. I.

FINITE DEFLECTIONS OF A RIGID  
VISCOPLASTIC STRAIN-HARDENING  
ANNULAR PLATE LOADED IMPULSIVELY

N. JONES

RECEIVED  
OCT 11 1967  
LIBRARY  
UNIVERSITY OF MICHIGAN

AD662399

Department of Defense  
Advanced Research Projects Agency  
Contract SD-86  
Materials Research Program

ARPA E53

October 1967

BU  
ARPA-E-53

FINITE DEFLECTIONS OF A RIGID VISCOPLASTIC STRAIN-HARDENING

ANNULAR PLATE LOADED IMPULSIVELY

by

Norman Jones\*

Abstract

A relatively simple analytical treatment of the behavior of a rigid-plastic annular plate subjected to an initial linear impulsive velocity profile is presented. The influence of finite-deflections has been included in addition to strain-hardening and strain-rate sensitivity of the plate material.

It is shown, for deflections up to the order of twice the plate thickness, that strain-hardening is unimportant, strain-rate sensitivity has somewhat more effect, while membrane forces play a dominant role in reducing the permanent deflections.

TECHNICAL LIBRARY  
BLDG 313  
ABERDEEN PROVING GROUND MD.  
STEAP-TL

---

\* Division of Engineering, Brown University

20060223358



## Notation

D	strain-rate sensitivity coefficient defined in equation (17)
E	modulus of elasticity
H	plate thickness
$M_o$	$\sigma_o H^2/4$
$M_r, M_\theta$	radial and circumferential bending moments per unit length
$N_o$	$\sigma_o H$
$N_r, N_\theta$	radial and circumferential membrane forces per unit length
Q	transverse shear force per unit length of plate
R	outside radius of plate
T	time at which plate reaches permanent position
$W_m$	maximum permanent deflection of plate
$V_o$	initial velocity of plate
a	inside radius of annular plate
e	ratio of the slopes of the elastic and plastic portions of a stress-strain curve
k	distributed pressure per unit area of undeformed plate
$m_r, m_\theta$	dimensionless bending moments $M_r/M_o, M_\theta/M_o$
$n_r, n_\theta$	dimensionless membrane forces $N_r/N_o, N_\theta/N_o$
p	strain-rate sensitivity coefficient defined in equation (17)
r	radial coordinate of plate
t	time
u	displacement in direction r of undeformed plate

Notation (continued)

w	transverse deflection perpendicular to undeformed plate
$\alpha$	$a/R$
$\beta$	$\left(\frac{HV_0}{2DR^2}\right)^{1/p}$
$\gamma$	$\nu H^2/R^2$
$\epsilon_r, \epsilon_\theta$	radial and circumferential strains
$\theta$	circumferential coordinate lying in plate
$\kappa_r, \kappa_\theta$	radial and circumferential curvatures
$\lambda$	$\frac{\mu V_0^2 R^2}{M_0 H}$
$\mu$	mass per unit area of plate
$\nu$	$\frac{E}{\sigma_0 e}$
$\sigma$	stress
$\sigma_0$	yield stress in simple tension
$\phi$	slope of the mid-plane of a plate measured in a plane which passes through $r = 0$ and is perpendicular to the plate surface
$\Delta$	$W_m/H$
$\Omega$	defined by equation (75)
$(\dot{\quad})$	$\frac{\partial}{\partial t} (\quad)$
$(\quad)'$	$\frac{\partial}{\partial r} (\quad)$

## 1. Introduction

It is apparent from a study of the current literature on the dynamic behavior of some simple rigid-plastic structures (e.g. beams and cantilevers [1]) that any strain-rate sensitivity which a material exhibits should be included in theoretical calculations, while strain-hardening may be disregarded unless the structure has a small length-to-thickness ratio [2,3]. Moreover, it has also been shown that it is essential to consider the influence of finite-deflections (i.e. membrane forces) in situations where axial restraints are present and deflections of the order of the beam thickness, or greater, are permitted [4].

Florence [5] examined the behavior of some simply supported circular plates when subjected to uniformly distributed impulses and observed permanent deflections which were considerably smaller than those predicted by a simple bending only theory [6]. Wierzbicki [7] in studying this problem recently examined the influence of strain-rate sensitivity of the material and presented a number of results for different viscosities, some of which are similar to the corresponding experimental values (Florence states that the material from which the plates were cut is believed to be somewhat insensitive to rate-of-strain). Further, Perrone [8] has examined the influence of strain-rate sensitivity on the behavior of a simply supported annular plate subjected to an initial velocity profile and has suggested an attractive method for analyzing structures which are loaded impulsively. However, it has been demonstrated recently that finite-deflections (i.e. membrane forces) play, as might be expected, a significant role in reducing the permanent deflections of plates loaded impulsively [9] or dynamically [10]

which leads one to suspect that the influence of strain-rate sensitivity may have been somewhat exaggerated in [7,8].

It is the object of this article, therefore, to study the combined influence of strain-rate sensitivity and strain-hardening on the finite deformation of rigid-plastic circular plates which are loaded dynamically. A conscious attempt is made to simplify the selected problem in accordance with the spirit of much of the previous work on simple structures, which has been aimed at preserving the appealing simplicity of rigid-plastic analyses, yet at the same time retaining the principal features of behavior. It is shown that the dynamic behavior of the annular plate illustrated in Fig. 1 can be described with fairly simple analytical expressions obtained by extending the ideas developed previously in references [2] and [9].

## 2. Equilibrium Equations

The equations of equilibrium in the tangential and transverse directions of the deformed element shown in Fig. 2 are [9]

$$rn_r' + n_r - n_\theta = -rkw'/N_o + \mu r\ddot{w}'/N_o + \mu r\ddot{u}/N_o \quad (1)$$

and

$$rm_r'' + 2m_r' - m_\theta' - 4n_\theta w'/H = rk/M_o - \mu r\ddot{w}/M_o + \mu r\ddot{u}w'/M_o \quad (2)$$

respectively, where

$$n_r, n_\theta = N_r/N_o, N_\theta/N_o$$

$$m_r, m_\theta = M_r/M_o, M_\theta/M_o$$

and the shear force  $Q$  has been eliminated using

$$rQ/M_0 = m_r + rm_r' - m_\theta \quad (3)$$

### 3. Strains and Curvatures

It may be shown for small strains [9,11] that

$$\epsilon_r = u' + w'^2/2 \quad (4)$$

$$\epsilon_\theta = u/r \quad (5)$$

$$\kappa_r = (1 + u')w'' - u''w' \quad (6)$$

and

$$\kappa_\theta = w'/r \quad (7)$$

from which

$$\dot{\epsilon}_r = \dot{u}' + w'\dot{w}' \quad (8)$$

$$\dot{\epsilon}_\theta = \dot{u}/r \quad (9)$$

$$\dot{\kappa}_r = (1 + u')\dot{w}'' + \dot{u}'w'' - \dot{u}''w' - u''\dot{w}' \quad (10)$$

and

$$\dot{\kappa}_\theta = \dot{w}'/r \quad (11)$$

The positive directions of  $u$  and  $w$  are indicated in Fig. 2.

### 4. Yield Condition

It has been found that disregarding elastic effects when analyzing cantilever beams loaded dynamically is a powerful simplification and a

valid approximation provided the external energy is at least three times larger than the strain energy absorbed by the beam at its elastic limit [3]. Consequently, in order to simplify the ensuing theoretical analysis, the material of the plate is assumed to remain rigid up to its yield point.

The yield condition proposed by Hodge [12] and illustrated in Fig. 3 will be used here since it simplifies considerably a previous approximate analysis, the results of which agree reasonably with experimental values recorded on plates loaded impulsively [9]. This approximate yield surface is an "upper" bound to the Tresca yield condition for a uniform shell [13], while a similar one 0.618 times as large provides a "lower" bound.

## 5. Constitutive Equations

The constitutive equations which were developed [2] in order to analyze the behavior of a rigid viscoplastic strain-hardening beam impulsively loaded will be used in this section to describe the influence of strain-hardening and strain-rate sensitivity on a linearized four-dimensional yield surface [12].

### 5.1 Strain-Hardening

Strain-hardening of the plate material is described by a linear relation of the form

$$\frac{\sigma}{\sigma_0} = 1 + v\varepsilon \quad (12)$$

where

$$v = \frac{E}{\sigma_0 e}$$



If it is assumed the yield surface [12] illustrated in Fig. 3 grows outward according to (12) as indicated in Fig. 4(a), then it may be shown that the following relations

$$n_{\theta} = 1 + \nu \epsilon_{\theta} , \quad \epsilon_{\theta} \geq 0 , \quad \epsilon_r = 0 , \quad 0 \leq n_r \leq 1 \quad (13)$$

$$n_r = 1 + \nu \epsilon_r , \quad \epsilon_r \geq 0 , \quad \epsilon_{\theta} = 0 , \quad 0 \leq n_{\theta} \leq 1 \quad (14)$$

$$m_{\theta} = 1 + \nu H \kappa_{\theta} / 3 , \quad \kappa_{\theta} \geq 0 , \quad \kappa_r = 0 , \quad 0 \leq m_r \leq 1 \quad (15)$$

and 
$$m_r = 1 + \nu H \kappa_r / 3 , \quad \kappa_r \geq 0 , \quad \kappa_{\theta} = 0 , \quad 0 \leq m_{\theta} \leq 1 \quad (16)$$

describe the behavior along the sides AB, BC, GH, and HJ, respectively.

Clearly, the relations for sides DE, EF, KL, and LM of the yield surface may be obtained from the corresponding equations (13)-(16) by noting the opposite directions of the forces, moments, strains and curvatures and modifying accordingly.

## 5.2 Strain-Rate Sensitivity

Cowper and Symonds [14] observed that a constitutive equation of the form

$$\frac{\sigma}{\sigma_0} = 1 + \left( \frac{\dot{\epsilon}}{D} \right)^{1/p} \quad (17)$$

could be fitted to the data of Manjoine provided  $D = 40.4 \text{ sec}^{-1}$  and  $p = 5$ . Thus, when the yield surface [12] grows with increase in strain and curvature rates as indicated in Fig. 4(b), it may be shown that the following expressions

$$n_{\theta} = 1 + \left(\frac{\dot{\epsilon}_{\theta}}{D}\right)^{1/p}, \quad \dot{\epsilon}_{\theta} \geq 0, \quad \dot{\epsilon}_r = 0, \quad 0 \leq n_r \leq 1 \quad (18)$$

$$n_r = 1 + \left(\frac{\dot{\epsilon}_r}{D}\right)^{1/p}, \quad \dot{\epsilon}_r \geq 0, \quad \dot{\epsilon}_{\theta} = 0, \quad 0 \leq n_{\theta} \leq 1 \quad (19)$$

$$m_{\theta} = 1 + \frac{2p}{2p+1} \left(\frac{H\dot{\kappa}_{\theta}}{2D}\right)^{1/p}, \quad \dot{\kappa}_{\theta} \geq 0, \quad \dot{\kappa}_r = 0, \quad 0 \leq m_r \leq 1 \quad (20)$$

and

$$m_r = 1 + \frac{2p}{2p+1} \left(\frac{H\dot{\kappa}_r}{2D}\right)^{1/p}, \quad \dot{\kappa}_r \geq 0, \quad \dot{\kappa}_{\theta} = 0, \quad 0 \leq m_{\theta} \leq 1 \quad (21)$$

describe the behavior along the sides AB, BC, GH, and HJ, respectively. Further, the relations for the sides DE, EF, KL, and LM of the yield surface may be easily obtained from (18)-(21).

### 5.3 Combined Strain-Hardening and Strain-Rate Sensitivity

Symonds [1] and Perrone [15] have suggested that

$$\frac{\sigma}{\sigma_0} = f(\epsilon)g(\dot{\epsilon}) \quad (22)$$

could be used to analyze structures loaded dynamically, where  $f(\epsilon)$  and  $g(\dot{\epsilon})$  are strain-hardening and strain-rate sensitive relations, respectively.

It is evident from equations (12,13,15,17,18,20) that when  $\epsilon_{\theta} \geq 0$ ,  $\dot{\epsilon}_{\theta} \geq 0$ ,  $\epsilon_r = \dot{\epsilon}_r = 0$ , and  $0 \leq n_r \leq 1$  (i.e. side AB of the yield surface), then according to (22)

$$n_{\theta} = 1 + v\epsilon_{\theta} + \left(\frac{\dot{\epsilon}_{\theta}}{D}\right)^{1/p} + v\epsilon_{\theta} \left(\frac{\dot{\epsilon}_{\theta}}{D}\right)^{1/p} \quad (23)$$

while for  $\kappa_{\theta} \geq 0$ ,  $\dot{\kappa}_{\theta} \geq 0$ ,  $\kappa_r = \dot{\kappa}_r = 0$ , and  $0 \leq m_r \leq 1$  (i.e. side GH of the yield surface),

$$m_{\theta} = 1 + \frac{vH\kappa_{\theta}}{3} + \frac{2p}{2p+1} \left(\frac{H\dot{\kappa}_{\theta}}{2D}\right)^{1/p} + \frac{2pvH\kappa_{\theta}}{3(2p+1)} \left(\frac{H\dot{\kappa}_{\theta}}{2D}\right)^{1/p} \quad (24)$$

The corresponding expressions for sides BC, DE, EF, HJ, KL and LM of the yield surface can be obtained from equations (13)-(22) in a similar manner. Clearly it is straightforward to obtain expressions for sides CD, FA, JK and MG, but these are not required here so are omitted for the sake of brevity.

## 6. Finite-Deformation of an Annular Plate Subjected to a Linearly Distributed Impulse

### 6.1 Rigid, Perfectly Plastic Material

In this section an examination is made of the behavior of a rigid, perfectly plastic annular plate which is subjected to a linearly distributed initial velocity profile of the form

$$\dot{w} = V_0 \frac{(R-r)}{(R-a)} \quad (25)$$

as indicated in Fig. 1.

Equation (25) suggests that the transverse displacements might be of the form

$$w = W(t) \frac{(R-r)}{(R-a)} \quad (26)$$

where  $W(t)$  is an unknown function of time.

Evidently it is more reasonable in this case to assume zero radial strain  $\epsilon_r$  rather than zero radial displacement  $u$ , a simplification which was helpful in previous analyses [4,9].

Thus, from (4)

$$u' = -w'^2/2 \quad (27)$$

which using (26) gives

$$u = \frac{W^2(R-r)}{2(R-a)^2} \quad (28)$$

It may be shown that the strain and curvature rates given by equations (8)-(11), (26) and (28) satisfy the normality requirements associated with the yield surface illustrated in Fig. 3 when

$$n_\theta = 1, \quad 0 \leq n_r \leq 1 \quad (29)$$

and

$$m_\theta = -1, \quad -1 \leq m_r \leq 0 \quad (30)$$

Substituting equations (29) and (30) into (2) with  $k = 0$  yields

$$\frac{\partial}{\partial r} (r^2 m_r') = 4rw'/H - \mu r^2 \ddot{w}/M_0 + \mu r^2 \ddot{u}w'/M_0 \quad (31)$$

which using (26) becomes

$$\frac{\partial}{\partial r} (r^2 m_r') = \frac{-4Wr}{H(R-a)} - \frac{\mu \ddot{w}(Rr^2 - r^3)}{M_0(R-a)}, \quad (32)$$

when  $\ddot{w} - \ddot{u}w' \approx \ddot{w}$ .

Integrating (32) twice with respect to  $r$  gives

$$m_r = \frac{-2W(r-a)^2}{H(R-a)r} - \frac{\mu \ddot{w}}{12M_0(R-a)r} (2Rr^3 - r^4 + 4Ra^3 - 3a^4 - 6Ra^2r + 4a^3r) + \frac{a}{r} - 1 \quad (33)$$

where the constants of integration have been evaluated from the conditions that  $m_r = Q = 0$  at  $r = a$ .

If the annular plate is simply supported at its outer edge, then an additional requirement is  $m_r = 0$  at  $r = R$ , or

$$\ddot{w} + n^2 w = -\delta \quad (34)$$

the solution of which is

$$W = A \cos nt + B \sin nt - \delta/n^2 \quad (35)$$

where

$$n^2 = \frac{24V_o^2}{\lambda H^2(1-\alpha)(1+3\alpha)} \quad (36)$$

$$\delta = n^2 H/2 \quad (37)$$

$$\lambda = \frac{\mu V_o^2 R^2}{M_o H} \quad (38)$$

and

$$\alpha = a/R \quad (39)$$

Now the initial values  $w = 0$  and  $\dot{w} = V_o \frac{(R-r)}{(R-a)}$  are satisfied by equation (35) when

$$A = \delta/n^2 \quad (40)$$

and

$$B = V_o/n \quad (41)$$

The motion of the plate ceases at  $t = T$  when  $\dot{W} = 0$ , where using (35), (40) and (41)

$$\tan nT = V_o n/\delta \quad (42)$$

The permanent shape of the plate is

$$\frac{w_m}{H} = \frac{1}{2(1-\alpha)} \left\{ \sqrt{1 + \frac{\lambda(1-\alpha)(1+3\alpha)}{6}} - 1 \right\} \left(1 - \frac{r}{R}\right) \quad (43)$$

However, in order to ensure  $m_r'$  remains positive at the outer edge of the plate, it is necessary that

$$\frac{W(t)}{H} \leq \frac{1+\alpha}{4\alpha} \quad (44)$$

Further, if  $n_r' \geq 0$  and  $n_r \leq 1$  at  $r = R$ , then equations (28) and (35) only satisfy equations (1) and (29) with  $n_r = 0$  at  $r = a$  provided

$$\lambda \leq \frac{24\alpha}{1+2\alpha} \left(\frac{R}{H}\right)^2 \quad (45)$$

Equation (45) is not as restrictive as equation (44) since  $R/H$  must be large in order for plate theory to be appropriate. If one is interested in deflections, the magnitude of which would violate the inequality (44), then it appears reasonable to consider the analysis outlined here as valid up to time  $t = \tau$  when  $m_r' = 0$  at  $r = R$ , while for  $\tau \leq t \leq T$  the plate could be considered to behave as a membrane.

For small values of the parameter  $\alpha$  ( $\ll 0.1$  approx.) it may be shown that  $m_r \geq -1$  demands a more severe limitation of the analysis than those imposed by either equations (44) or (45).

If the deflections of the plate are assumed to be infinitesimal, then  $n_r = n_\theta = 0$  and an analysis similar to the one outlined above gives equation (34) without the  $n^2W$  term. The permanent shape of the plate for this case may be shown to be

$$\frac{W_m}{H} = \frac{\lambda(1+3\alpha)}{24} \left(1 - \frac{r}{R}\right) \quad (46)$$

which agrees with the bending only solution for the same problem presented by Perrone [8].

It is evident from Fig. 5 that when finite deflections are permitted, then the consideration of membrane forces in addition to bending moments (43) leads to significantly smaller permanent deformations than those predicted by a simple bending moment only theory (46).

6.2 Rigid, Strain-Hardening Material

When utilizing the linear transverse displacement profile (26) and the condition for zero radial strain (27), it may be shown that  $\epsilon_r = \dot{\epsilon}_r = \kappa_r = \dot{\kappa}_r = 0$ ,  $\epsilon_\theta \geq 0$ ,  $\dot{\epsilon}_\theta \geq 0$ ,  $\kappa_\theta \leq 0$ , and  $\dot{\kappa}_\theta \leq 0$ . These strain and curvature rates satisfy the normality requirements associated with the yield surface [12] shown in Fig. 3 and developed in section 5.1 provided

$$n_\theta = 1 + \nu \epsilon_\theta, \quad 0 \leq n_r \leq 1 \quad (47)$$

and

$$m_\theta = -1 + \nu H \kappa_\theta / 3, \quad -1 \leq m_r \leq 0 \quad (48)$$

Making use of equations (5,7,26,28,47 and 48) permits equation (2) to be written

$$\frac{\partial}{\partial r} (r^2 m_r') = \frac{\nu HW}{3(R-a)r} - \frac{4Wr}{H(R-a)} - \frac{2\nu W^3(R-r)}{H(R-a)^3} - \frac{\mu \ddot{w}(Rr^2-r^3)}{M_o(R-a)} \quad (49)$$

when neglecting  $\ddot{w}'$  compared with  $\ddot{w}$ .

Thus,

$$\begin{aligned} m_r = & \frac{\nu HW}{3(R-a)ar} (a \log_e(a/r) + r - a) - \frac{2W(r-a)^2}{H(R-a)r} - \\ & - \frac{\nu W^3}{H(R-a)^3 r} (2Rr \log_e(r/a) - r^2 + 2ar + 2aR - 2Rr - a^2) - \\ & - \frac{\mu \ddot{w}}{12M_o(R-a)r} (2Rr^3 - 6Ra^2r - r^4 + 4a^3r + 4Ra^3 - 3a^4) + \\ & + \frac{a}{r} - 1 + \frac{\nu HW}{3(R-a)ar} (a-r) \end{aligned} \quad (50)$$

where the constants of integration have been evaluated from the requirements that  $m_r = Q = 0$  at  $r = a$ .

Now in order to give  $m_r = 0$  at  $r = R$ ,

$$a_1 \ddot{W} + b_1 W^3 + c_1 W = d_1 \quad (51)$$

where

$$a_1 = -(1-\alpha)/\delta \quad (52)$$

$$b_1 = - \frac{\gamma \{4\alpha - \alpha^2 - 3 + 2 \log_e(1/\alpha)\}}{H^3(1-\alpha)^3} \quad (53)$$

$$c_1 = \frac{\gamma \log_e \alpha}{3H(1-\alpha)} - \frac{2(1-\alpha)}{H} \quad (54)$$

$$d_1 = 1 - \alpha \quad (55)$$

and

$$\gamma = \nu H^2 / R^2 \quad (56)$$

If  $y = \dot{W}^2$ , equation (51) can be rewritten in the form

$$\frac{dy}{dW} = \frac{-2b_1 W^3}{a_1} - \frac{2c_1 W}{a_1} - 2\delta \quad (57)$$

from which

$$y = - \frac{b_1 W^4}{2a_1} - \frac{c_1 W^2}{a_1} - 2\delta W + V_o^2 \quad (58)$$

where the constant of integration has been evaluated from the requirement

that  $y = V_o^2$  and  $W = 0$  when  $t = 0$ .

Furthermore, the velocity  $\dot{W}$  is zero when the displacement  $W$  reaches its final value  $W_{\max}$ . Thus, from (58)

$$b_1 H^3 \Delta^4 + 2c_1 H \Delta^2 - 4d_1 \Delta - 2a_1 V_o^2 / H = 0 \quad (59)$$

where

$$\Delta = W_{\max} / H \quad (60)$$



For a given value of  $\alpha$  and  $\gamma$ , it is simpler to substitute known values of  $\Delta$  into (59) and evaluate the associated magnitude of  $\lambda$  from a linear equation rather than solve a quartic equation for  $\Delta$  corresponding to a given value of  $\lambda$ .

If  $\gamma = 0$ , equation (59) reduces to the rigid-plastic case given by (43) while if  $\gamma = c_1 = 0$ , then it further degenerates to the bending only solution (46).

In order for the above theory to remain valid, it is necessary that  $m_r' \geq 0$  at  $r = R$  or

$$\Delta \left[ 4\alpha + \frac{\gamma(1+3\alpha)}{3(1-\alpha)} \left\{ 1 + \frac{2(1+2\alpha)\log_e \alpha}{(1-\alpha)(1+3\alpha)} \right\} \right] + \frac{\gamma\Delta^3}{(1-\alpha)^4} \{ 2(2 + \alpha - 2\alpha^2 - \alpha^3) + 2 \log_e \alpha(1 + 2\alpha + 3\alpha^2) \} \leq 1 + \alpha \quad (61)$$

Furthermore, if equation (1) is solved using equations (5,26,28 and 47) and the condition that  $n_r = 0$  at  $r = a$ , then in order to maintain  $n_r \leq 1$  and  $n_r' \geq 0$  at  $r = R$  it is found that the solution is restricted to deflections

$$\Delta^2 \leq \frac{2\alpha(1-\alpha)^2}{\gamma(\alpha-1-\log_e \alpha)} \quad (62)$$

### 6.3 Rigid, Viscoplastic Material

Perrone [8] has shown for some simple structures loaded impulsively and made from a strain-rate sensitive material that excellent agreement with exact solutions may be obtained when utilizing a strain-rate insensitive material with a constant yield stress equal to the initial dynamic yield stress.

Now it may be shown using equations (8)-(11), (26) and (28) that

$$\dot{\epsilon}_r = \dot{\kappa}_r = 0 \quad (63)$$

$$\dot{\epsilon}_{\theta} = \frac{W\dot{W}(R-r)}{(R-a)^2 r} \quad (64)$$

and

$$\dot{\kappa}_{\theta} = \frac{-\dot{W}}{(R-a)r} \quad (65)$$

However, if Perrone's simplification is used, then (63)-(65) become

$$\dot{\epsilon}_r = \dot{\kappa}_r = \dot{\epsilon}_{\theta} = 0 \quad (66)$$

and

$$\dot{\kappa}_{\theta} = \frac{-V_o}{(R-a)r} \quad (67)$$

since  $W = 0$  and  $\dot{W} = V_o$  when  $t = 0$ .

Equations (66) and (67) are consistent with the yield surface shown in Fig. 3 and discussed in section 5.2 when

$$n_{\theta} = 1, \quad 0 \leq n_r \leq 1 \quad (68)$$

and

$$m_{\theta} = -1 - \frac{2p}{2p+1} \left( \frac{HV_o}{2Dr(R-a)} \right)^{1/p}, \quad -1 \leq m_r \leq 0 \quad (69)$$

Substituting equations (26,68 and 69) into (2) gives

$$\frac{\partial}{\partial r} (r^2 m_r') = \frac{2}{2p+1} \left( \frac{HV_o}{2D(R-a)} \right)^{1/p} r^{-1/p} - \frac{4Wr}{H(R-a)} - \frac{\mu \ddot{W}(Rr^2 - r^3)}{M_o(R-a)} \quad (70)$$

Integrating (70) and ensuring that  $m_r = Q = 0$  at  $r = a$  gives an equation in  $m_r$  which in order to remain zero at the simply supported outer edge yields

$$\ddot{W} + n^2 W = d_2 \quad (71)$$

where

$$d_2 = -c_2/a_1 \quad (72)$$

$$c_2 = (\Omega-1)(1-\alpha) \quad (73)$$

$$\beta = \left( \frac{HV_o}{2DR^2} \right)^{1/p} \quad (74)$$

and

$$\Omega = \frac{2p^2\beta(\alpha^{1-1/p}-1)}{(2p+1)(p-1)(1-\alpha)^{1+1/p}} \quad (75)$$

The solution of (71) is

$$w = \frac{-d_2}{n^2} \cos nt + \frac{V_o}{n} \sin nt + \frac{d_2}{n^2} \quad (76)$$

where the constants of integration have been determined from the initial conditions  $w = 0$  and  $\dot{w} = V_o$ .

Now the motion of the plate ceases at  $t = T$  when  $\dot{w} = 0$ . Thus using (76) it may be shown that

$$\tan nT = -V_o n/d_2, \quad (77)$$

and the permanent shape of the plate is

$$\frac{w_m}{H} = \frac{(1-\Omega)}{2(1-\alpha)} \left\{ \sqrt{1 + \frac{(1-\alpha)(1+3\alpha)\lambda}{6(1-\Omega)^2}} - 1 \right\} \left( 1 - \frac{r}{R} \right) \quad (78)$$

The foregoing analysis is valid provided  $m_r' \geq 0$  at  $r = R$ , or

$$4\alpha\Delta - \frac{2p\beta[1-3\alpha^2+2\alpha+p\{1+3\alpha^2+2\alpha-2\alpha^{1-1/p}(1+2\alpha)\}]}{(2p+1)(p-1)(1-\alpha)^{1+1/p}} \leq 1 + \alpha \quad (79)$$

Further, in order that  $n_r \leq 1$  and  $n_r' \geq 0$  at  $r = R$  the inequality (45) must also be satisfied. However, for small values of  $\alpha$  ( $< 0.1$  approx.) and large values of  $\beta$  ( $> 0.5$  approx.) it may be shown that another more restrictive inequality exists for the requirement  $m_r \geq -1$ .

If the variation of  $\dot{\kappa}_\theta$  with time given by equation (65) is retained in the foregoing analysis instead of its simplified version (67), it may be

shown that the equation corresponding to (71) can be solved with a series solution somewhat similar to the one used by Perrone [8]. The maximum deflections predicted in this case are found to be in almost total agreement with (78) when retaining only the first three terms in the rapidly convergent series. These results further support Perrone's observations [8] and indicate that they are also valid, as might be expected, for finite-deflections. It is important to point out here, however, that no account has been taken of any strain-rate sensitivity which may arise from  $n_\theta$ .

#### 6.4 Rigid Strain-Hardening Viscoplastic Material

In this section the combined influence of strain-hardening and strain-rate sensitivity on the finite-deflections of a rigid-plastic annular plate will be examined by amalgamating the separate effects treated in sections 6.2 and 6.3 in the manner suggested in section 5.3.

It may be shown that the strain and curvature rates associated with the displacement profile (26) and the condition for zero radial strain (27) satisfy the normality requirements demanded by the yield surface illustrated in Fig. 3 and discussed in section 5.3 when

$$n_\theta = 1 + \frac{vW^2(R-r)}{2r(R-a)^2}, \quad \text{with } 0 \leq n_r \leq 1 \quad (80)$$

and

$$m_\theta = -1 - \frac{vHW}{3r(R-a)} - \frac{2p}{(2p+1)} \left( \frac{HV_o}{2D(R-a)r} \right)^{1/p} - \frac{2pvHW}{3(2p+1)(R-a)r} \left( \frac{HV_o}{2D(R-a)r} \right)^{1/p}$$

with  $-1 \leq m_r \leq 0$  (81)

If the equilibrium equation (2) is solved using equations (26,80 and 81) subject to the boundary conditions  $m_r = 0 = 0$  at  $r = a$ ,

it may be shown that in order for the radial bending moment to be zero at  $r = R$ , then

$$a_1 \ddot{W} + b_3 W + b_1 W^3 = -c_2 \quad (82)$$

where

$$b_3 = c_1 + \frac{2\gamma p^2 \beta (1-\alpha)^{-1/p}}{3H(2p+1)(1-\alpha)^{1+1/p}} \quad (83)$$

By making a variable change  $y = \dot{W}^2$ , equation (82) may be transformed to a first order differential equation which upon integration gives

$$y = \frac{-b_3 W^2}{a_1} - \frac{b_1 W^4}{2a_1} - \frac{2c_2 W}{a_1} + V_o^2 \quad (84)$$

where the constant of integration has been obtained from the initial condition  $y = V_o^2$  when  $t = 0$ .

It may be shown that the permanent deflection of the plate satisfies the quartic equation

$$b_1 H^3 \Delta^4 + 2b_3 H \Delta^2 + 4c_2 \Delta - 2a_1 V_o^2 / H = 0 \quad (85)$$

Equation (85) may be reduced to the results of sections 6.1-6.3 when  $\gamma = \beta = 0$ ,  $\beta = 0$ , and  $\gamma = 0$ , respectively.

## 7. Discussion

The results plotted in Fig. 5 illustrate the profound effect which membrane forces have on the behavior of annular plates loaded impulsively. This outcome is not unexpected and has been recently discussed elsewhere [9,10,16].

It is evident from the curves drawn in Fig. 6 that within the range of deflections examined, any material strain-hardening hardly reduces the

permanent deflections below those predicted by a rigid, perfectly plastic theory. If for mild steel  $\nu = 6$ , then  $\gamma = 0.06$  would refer to a mild steel plate with  $H/R = 1/10$  while  $\gamma = 0.015$  would correspond to  $H/R = 1/20$ . Clearly, strain-hardening has less effect for smaller values  $H/R$ .

Figure 7 indicates, as might be expected [1,2], that strain-rate sensitivity of a material gives rise to a "size effect," which means that physically smaller plates are more susceptible to rate-effects than larger ones. In Figure 7 the values  $\beta = 0.30$  and  $\beta = 0.70$  for annular plates ( $\alpha = 1/8$ ) made from mild steel with  $D = 40.4 \text{ sec}^{-1}$  and  $p = 5$ , correspond roughly to maximum strain rates of  $1 \text{ sec}^{-1}$  and  $60 \text{ sec}^{-1}$ , respectively. However, although it is clear from Figs. 6 and 7 that strain-rate effects are more important than material strain-hardening, they still have a surprisingly small influence when compared with the reduction of deflections arising from the action of membrane forces alone. It is evident from Fig. 8 that plates made from materials which exhibit strain-hardening and rate-effects could be treated as rigid-viscoplastic without strain-hardening. Even using a rigid, perfectly plastic material would introduce tolerable errors provided membrane forces were included. This observation might indicate why the results predicted by the rigid, perfectly plastic analysis for an impulsively load circular plate [9] were quite close to the corresponding experimental values [5].

In order to analyze plates with deflections larger than those permitted by the various inequalities stated in section 6, it appears reasonable to let the plate behave as outlined here until the time at which the particular inequality is violated then treat any subsequent behavior as membrane.

## 8. Conclusions

Herein is presented a relatively simple analytical treatment of the behavior of a rigid-plastic annular plate subjected to an initial linear impulsive velocity profile. The influence of finite-deflections has been included in addition to strain-hardening and strain-rate sensitivity of the plate material.

It is shown for deflections up to the order of twice the total plate thickness that strain-hardening is unimportant, strain-rate sensitivity has somewhat more effect, while membrane forces play a dominant role in reducing the permanent deflections. It is believed, therefore, that the results here with those of references [2,3] on beams indicate that a rigid-viscoplastic material without strain-hardening is suitable for analyzing dynamic problems.

## Acknowledgments

The work reported herein was supported by the Advanced Research Projects Agency, Department of Defense, under contract number SD-86 awarded to Brown University.

The author wishes to take this opportunity to express his appreciation to Miss E. Cerutti for computing the final results and to the National Science Foundation (Grant Number GP-4825) for making funds available to cover the costs of machine time.

References

1. Symonds, P. S., "Viscoplastic Behavior in Response of Structures to Dynamic Loading," Behavior of Materials Under Dynamic Loading, Ed. by N. J. Huffington, publ. by ASME, pp. 106-124, 1965.
2. Jones, N., "Influence of Strain-Hardening and Strain-Rate Sensitivity on the Permanent Deformation of Impulsively Loaded Rigid-Plastic Beams," to appear in *Int. J. Mech. Sci.*
3. Bodner, S. R., and Symonds, P. S., "Experimental and Theoretical Investigation of the Plastic Deformation of Cantilever Beams Subjected to Impulsive Loading," *Jnl. App. Mechs.*, Vol. 29, No. 4, pp. 719-728, 1962.
4. Symonds, P. S., and Mentel, T. J., "Impulsive Loading of Plastic Beams with Axial Constraints," *Jnl. Mech. Phys. Solids*, Vol. 6, pp. 186-202, 1958.
5. Florence, A. L., "Circular Plate Under a Uniformly Distributed Impulse," *Int. J. Solids Structures*, Vol. 2, pp. 37-47, 1966.
6. Wang, A. J., "The Permanent Deflection of a Plastic Plate Under Blast Loading," *Jnl. App. Mech.*, Vol. 22, pp. 375-376, 1955.
7. Wierzbicki, T., "Impulsive Loading of Rigid Viscoplastic Plates," *Int. J. Solids Structures*, Vol. 3, No. 4, pp. 635-647, 1967.
8. Perrone, N., "Impulsively Loaded Strain-Rate-Sensitive Plates," *Jnl. App. Mech.*, Vol. 34, No. 2, pp. 380-384, 1967.
9. Jones, N., "Impulsive Loading of a Simply Supported Rigid-Plastic Circular Plate," *Jnl. App. Mech.*, Paper No. 67-WA/APM-27.
10. Jones, N., "Finite Deflections of a Simply Supported Rigid-Plastic Circular Plate Loaded Dynamically," to appear in *Int. J. Solids and Structures*.
11. Reissner, E., "On Finite Deflections of Circular Plates," *Proc. Symposia App. Math.*, Vol. 1, pp. 213-219, 1949.
12. Hodge, P. G., "Yield Conditions for Rotationally Symmetric Shells Under Axisymmetric Loading," *Jnl. App. Mech.*, Vol. 27, No. 2, *Trans. ASME, Series 2*, pp. 323-331, 1960.
13. Onat, E. T., and Prager, W., "Limit Analysis of Shells of Revolution," Parts I and II, *Proc. Royal Netherlands Acad. of Sci.*, Vol. B57, pp. 534-541 and 542-548, 1954.



14. Cowper, G. R., and Symonds, P. S., "Strain-Hardening and Strain-Rate Effects in the Impact Loading of Cantilever Beams," Tech. Report No. 28, O.N.R., Div. of App. Math., Brown University, Sept. 1957.
15. Perrone, N., "A Mathematically Tractable Model of Strain-Hardening, Rate-Sensitive Plastic Flow," Jnl. App. Mech., Vol. 33, No. 1, pp. 210-211, 1966.
16. Florence, A. L., "Annular Plate Under a Transverse Line Impulse," AIAA Jnl., Vol. 3, No. 9, pp. 1726-1732, 1965.

### Titles of Figures

- Figure 1 - Annular Plate
- Figure 2 - Element of Plate
- Figure 3 - Yield Condition after Hodge [12]
- Figure 4 - (a) Rigid, Strain Hardening Yield Condition  
(b) Rigid, Strain-Rate Sensitive Yield Condition
- Figure 5 - Influence of Membrane Forces on the Final Deflection of a Simply Supported Annular Rigid, Perfectly Plastic Plate Subjected to a Linearly Distributed Impulse
- Figure 6 - Influence of Material Strain-Hardening
- Figure 7 - Influence of Material Strain-Rate Sensitivity
- Figure 8 - Combined Influence of Strain-Hardening and Strain-Rate Sensitivity

LINEAR INITIAL VELOCITY PROFILE

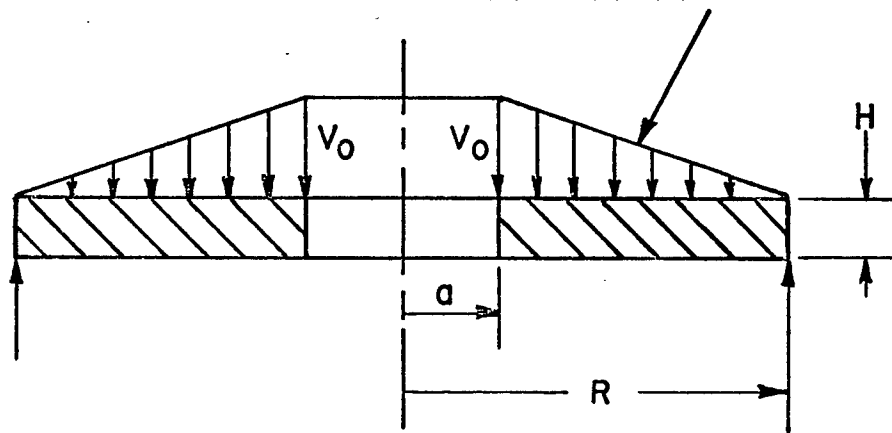


FIGURE I

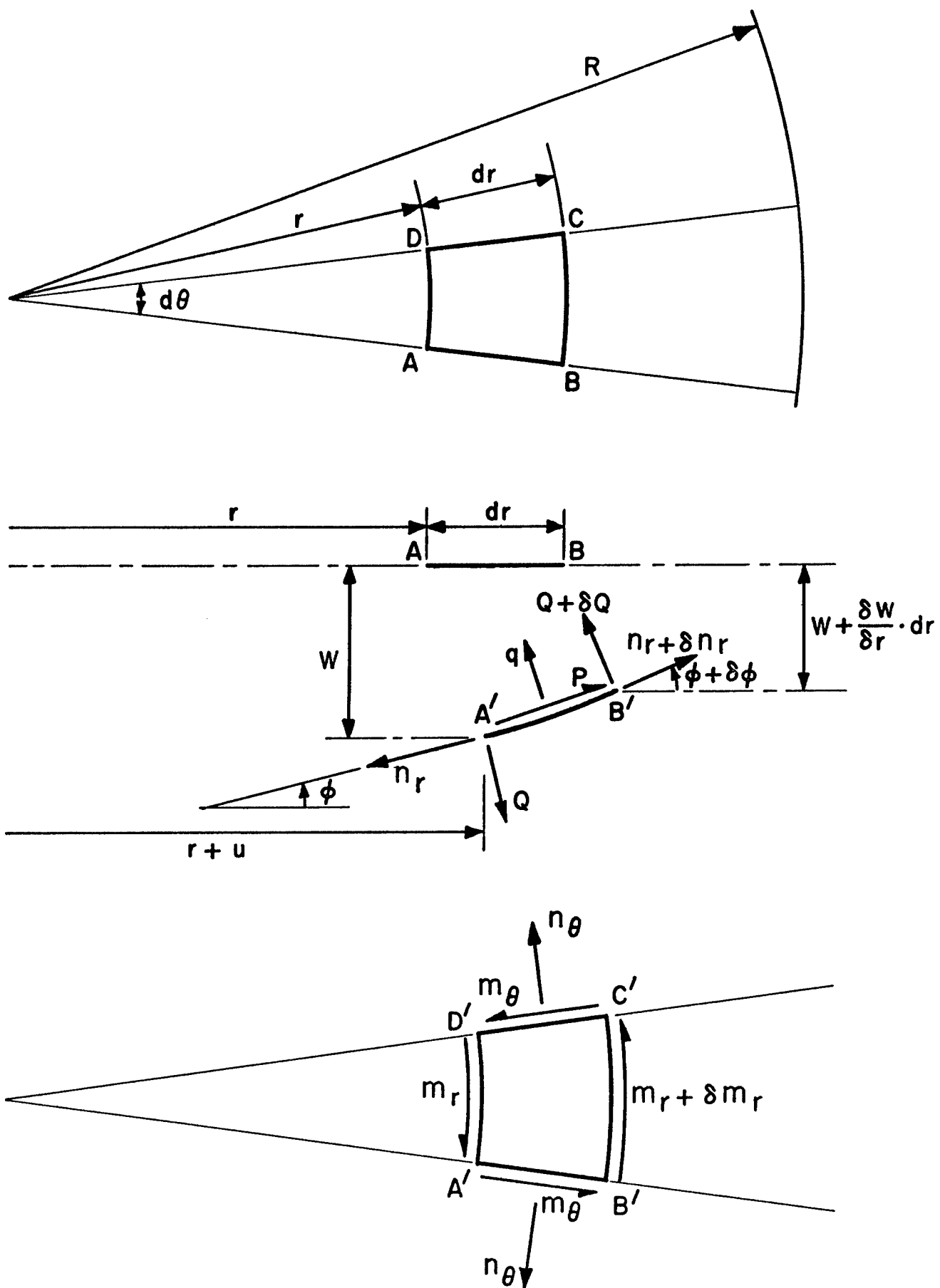


FIG. 2

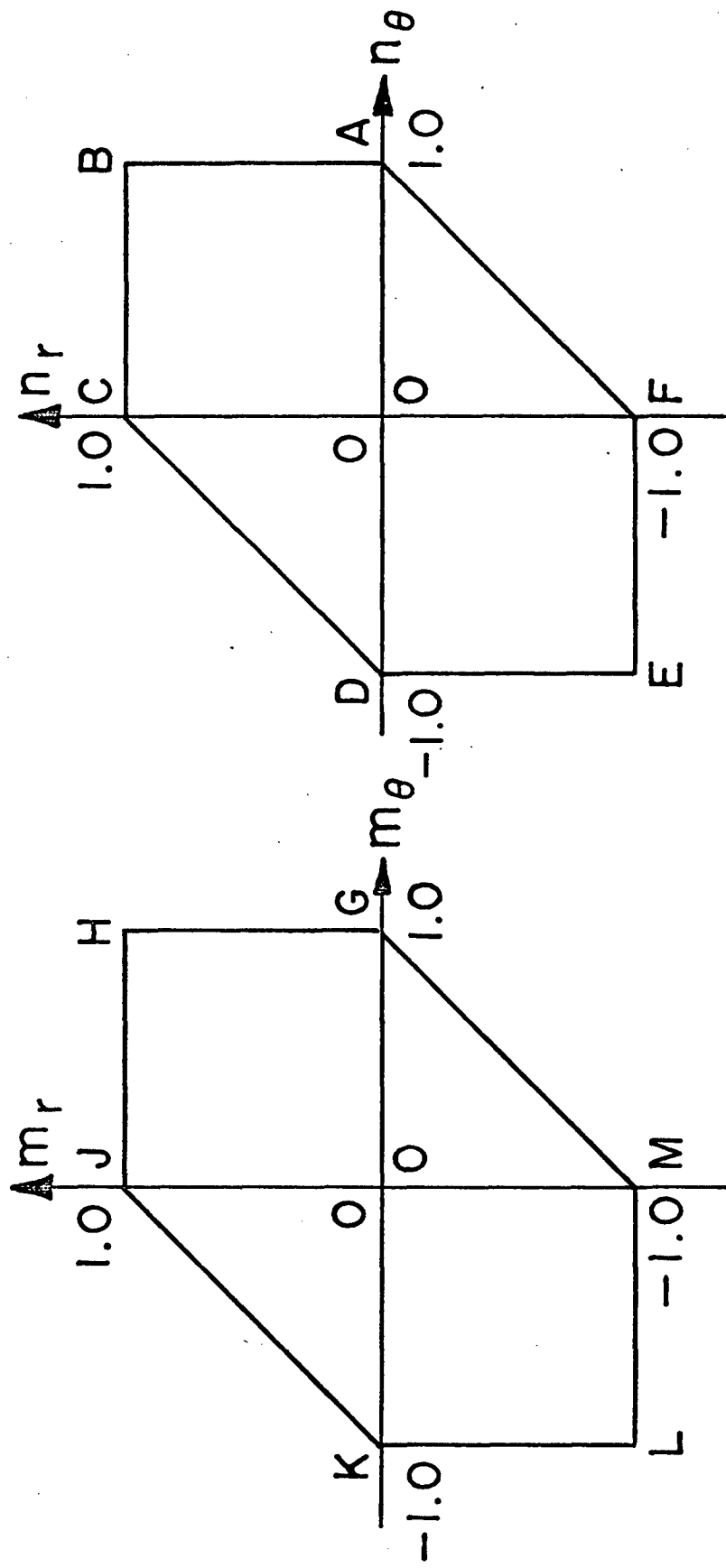
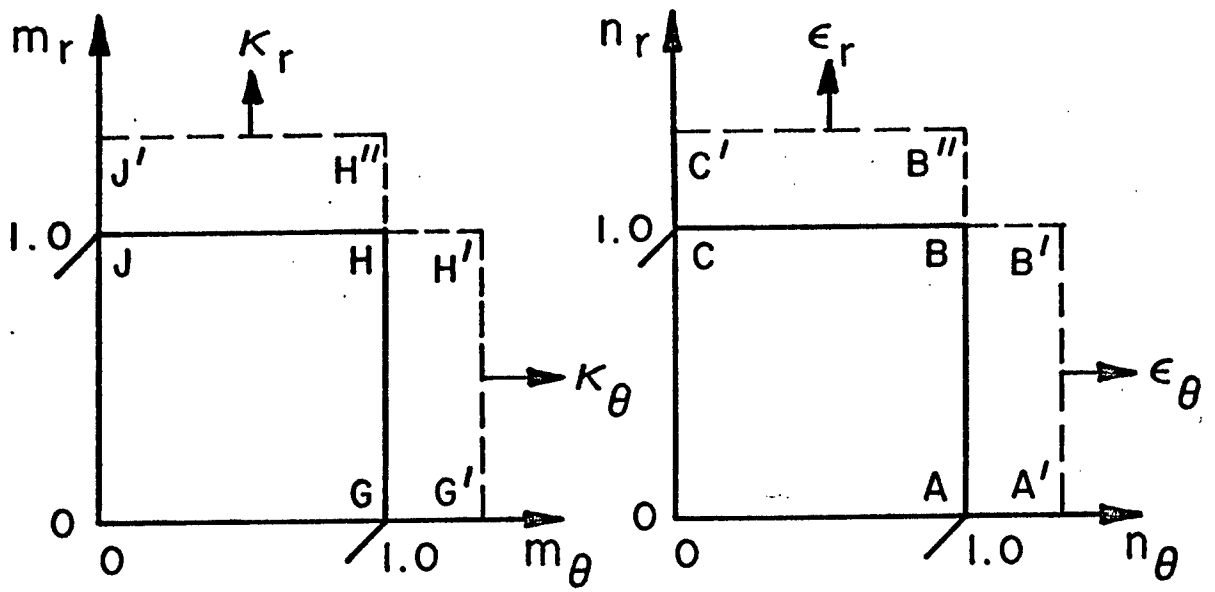
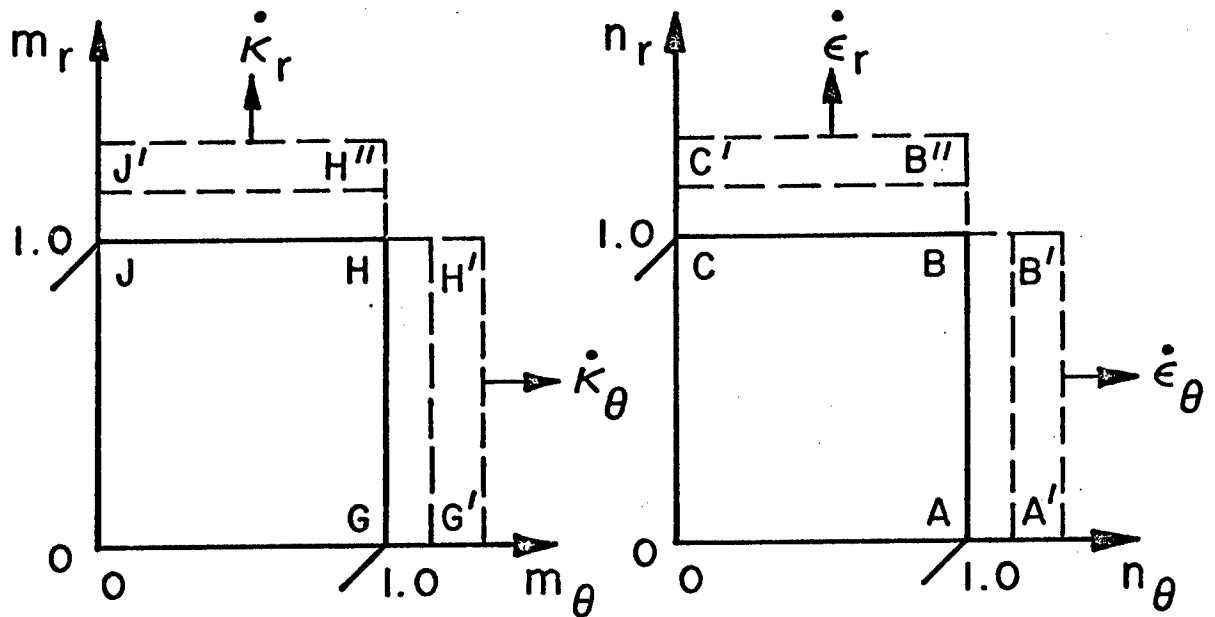


FIGURE 3



(a)



(b)

FIGURE 4

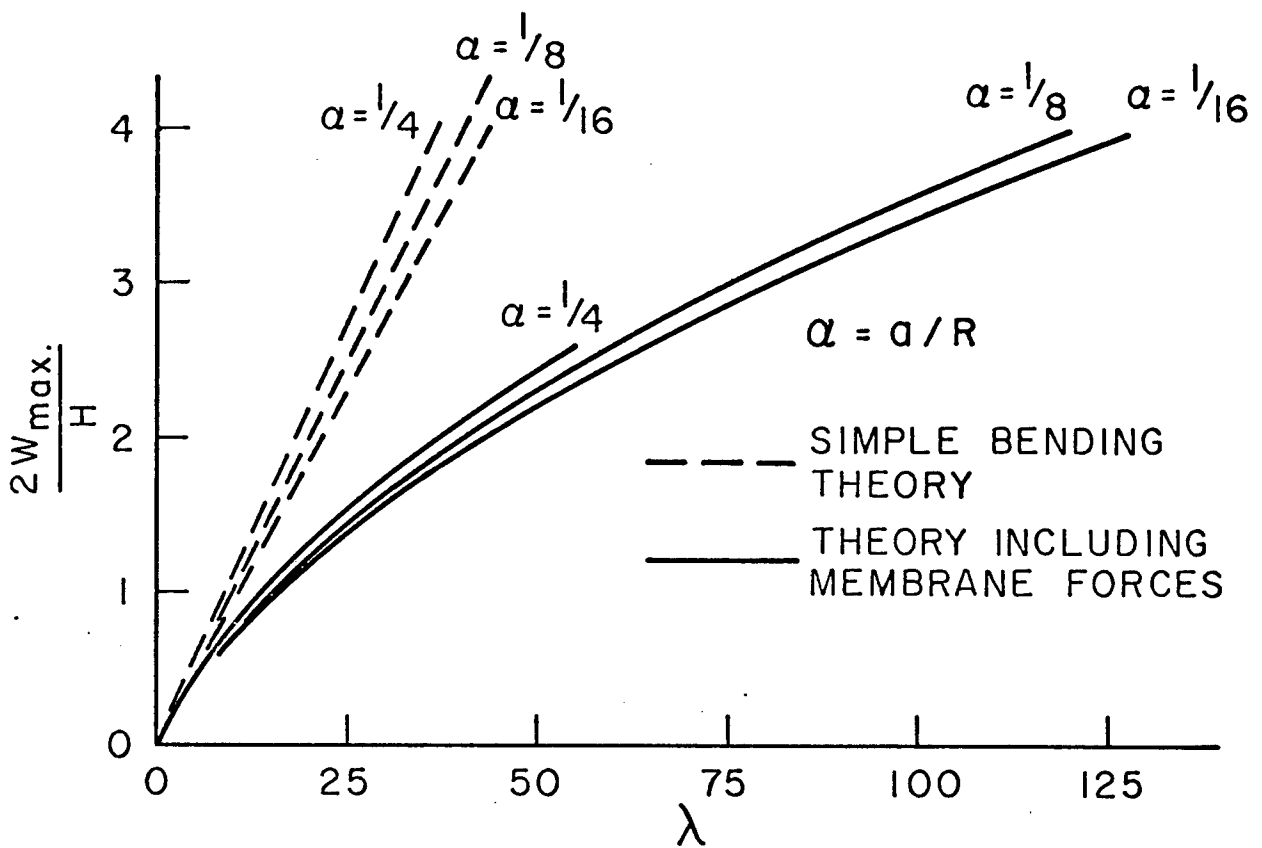


FIGURE 5

$$\alpha = 1/8$$

$$\beta = 0$$

$$\gamma = \nu H^2 / R^2$$

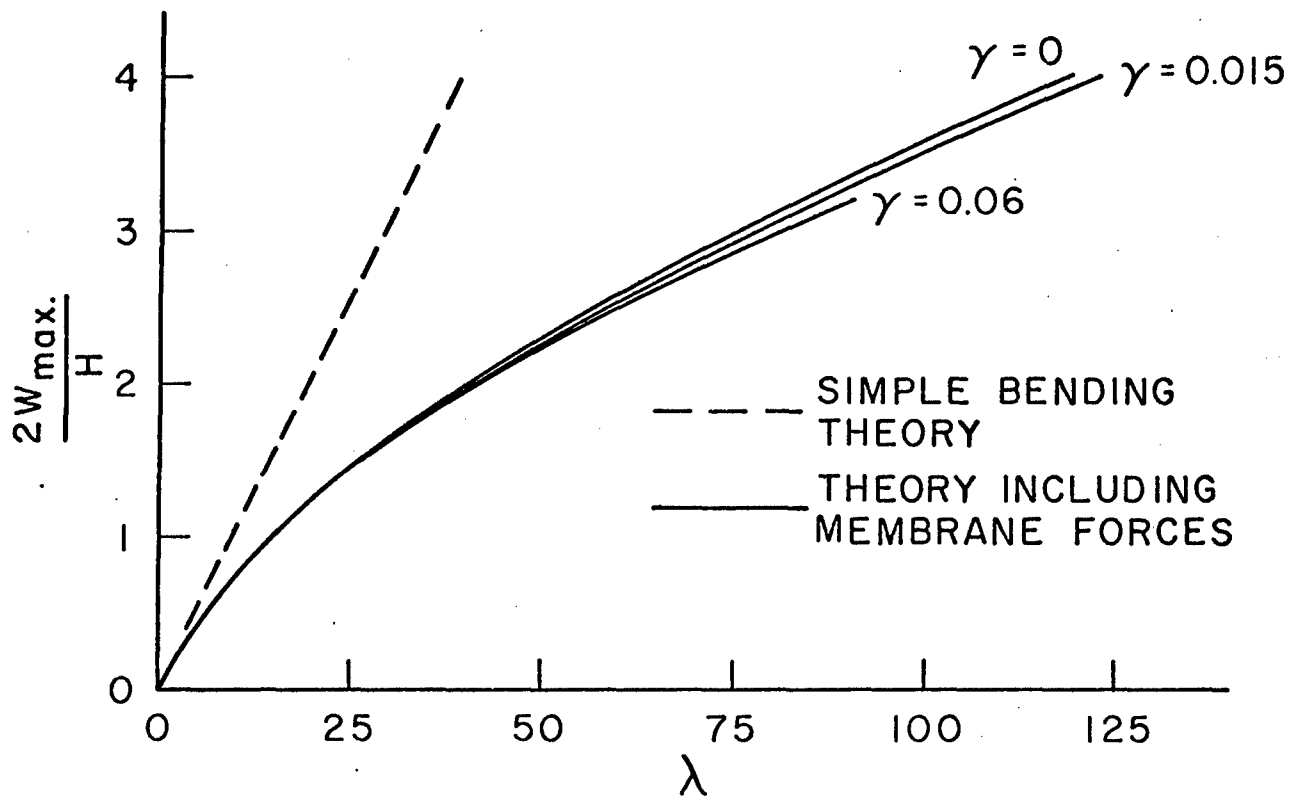


FIGURE 6



$$\alpha = 1/8$$

$$\beta = \left( \frac{HV_0}{2DR^2} \right)^{1/p}$$

$$\gamma = 0$$

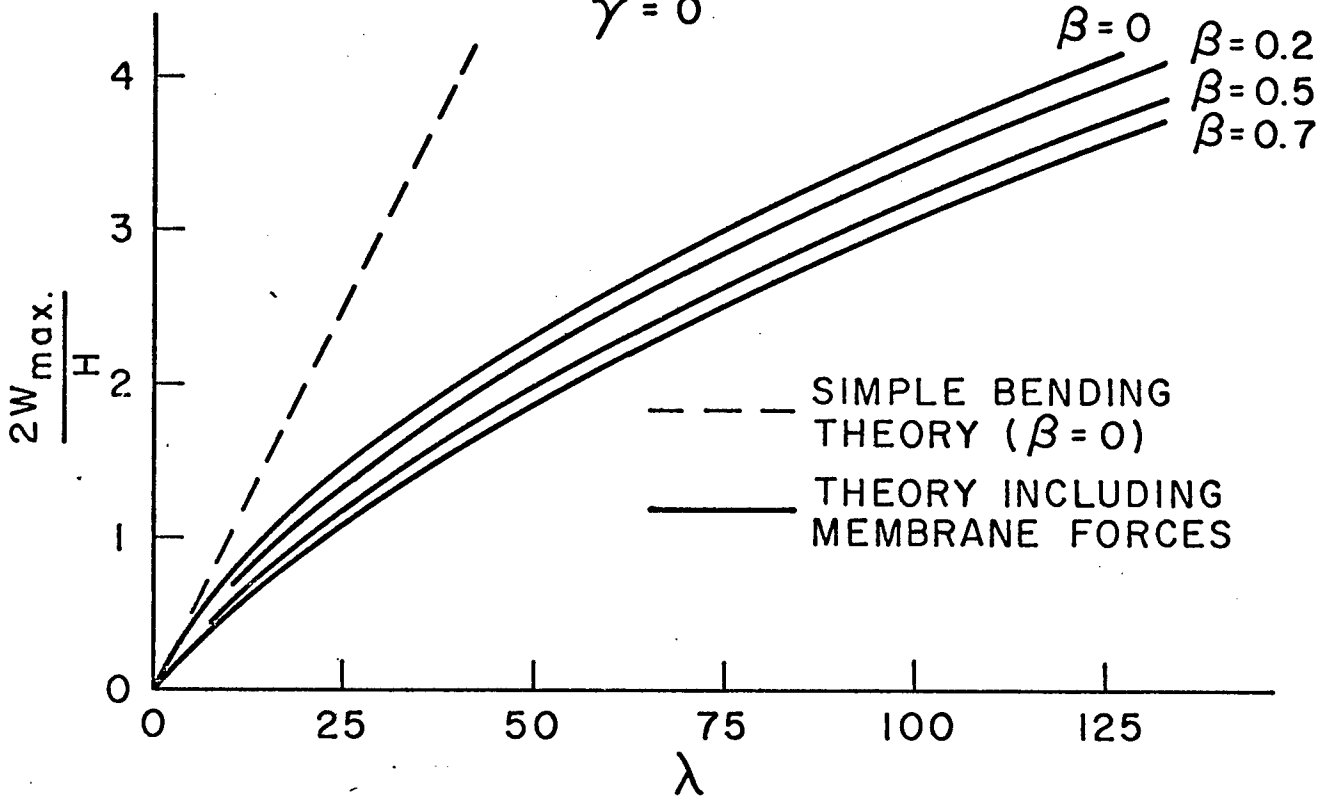


FIGURE 7

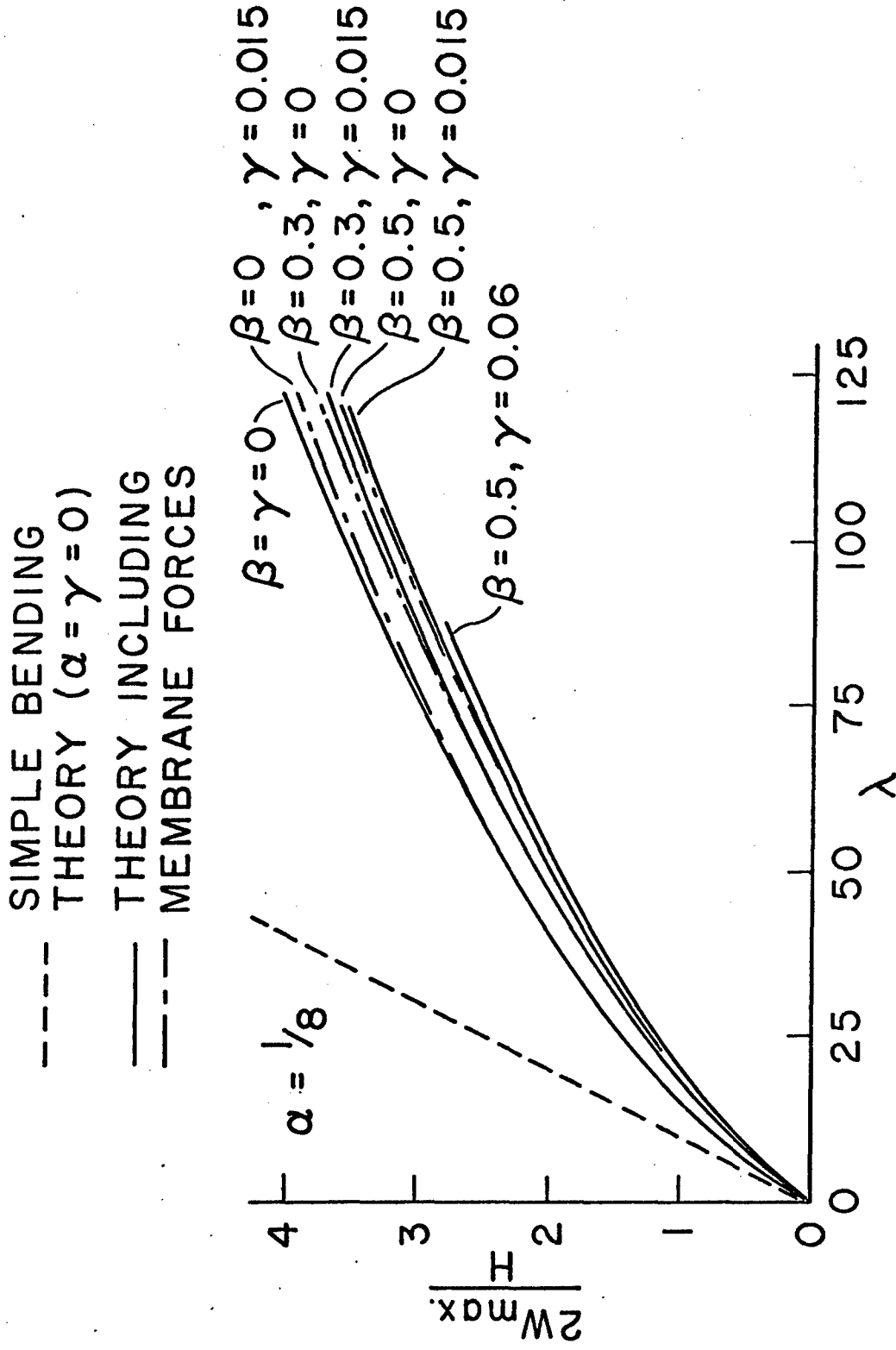


FIGURE 8